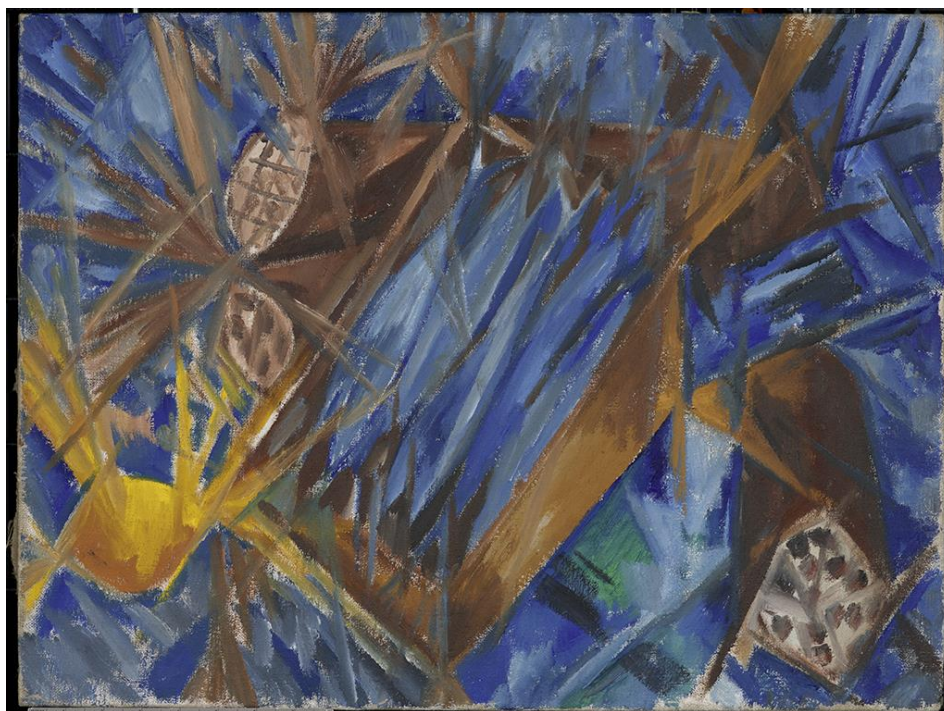


ANALYTICAL REPORT

[Ref.: AAR0955.L / 8 May 2018]



Rayonistic Sausage and Mackerel, 1912
Mikhail Larionov
Collection Museum Ludwig, Cologne, Inv. ML 1307

Art Analysis & Research Inc.
Ground Floor West, 162-164 Abbey Street, London SE1 2AN
T: +44 (0) 20 7064 1433
VAT Reg. No. 252 4541 22



Summary

A painting on canvas by Mikhail Larionov known as *Rayonistic Sausage and Mackerel (Saucisson et maquereaux rayonnistes)*, belonging to the Museum Ludwig (reference: ML 1307), was examined and analysed by Art Analysis & Research, Ltd. in cooperation with the Museum Ludwig, and funded through a grant from The Russian Avant Garde Research Project (RARP). It is thought to have been created in 1912 (it is not dated). This artwork formed a part of a group of fourteen well-provenanced paintings by the Russian artist couple Natalia Goncharova and Mikhail Larionov, held in the collection of the Museum Ludwig that comprised the focus of this work. The goal set for this research was to investigate these paintings in order to characterise similarities and differences, with the objectives of 1) providing detailed studies of the specific paintings, 2) obtaining wider information on the artists' methods, 3) defining a blueprint for promising methodologies to develop further on other works by these artists and with an aim of applying such information in support a *catalogue raisonné*, and 4) creating a foundation for applying similar methodologies and techniques to other artists of the genre. To this end, each of the paintings are described in individual reports (as here) accompanied by a summary report under separate cover. The results of the program of examination, material analysis and technical imaging will be set out herein.



Contents

Summary	2
Tables, Figures and Plates.....	4
A. Introduction.....	6
B. Examination, imaging and analysis of the images	7
B.1 Methodology	7
B.2 General observations	8
B.3 Imaging.....	8
B.3.i Photography with ultraviolet illumination	8
B.3.ii Short-wave infrared (SWIR)	9
B.3.iii X-radiography and weave analysis	9
C. Sampling and analysis	10
C.1 Introduction	10
C.2 Support	11
C.3 Radiocarbon dating.....	11
C.4 Ground.....	11
C.5 Underdrawing.....	12
C.6 Paint layers: Pigments	12
C.7 Paint layers: Binding media	12
C.8 Stratigraphy	12
D. Discussion of the findings	13
D.1 Support, ground and preparatory work	13
D.1.i The support	13
D.1.ii Priming.....	14
D.1.iii Underdrawing	14
D.2 Paint, pigments and binding media	14
D.2.i General observations.....	14
D.2.ii Paint: pigment and binding medium	15
D.2.iii Materials analysis and implications for dating	16
E. Conclusions	16
F. Acknowledgements.....	17
G. Appendices.....	18
App.1 Sampling and sample preparation	18

App.1.i Sampling	18
App.1.ii Cross-sectional analysis	19
App.2 Materials analysis summary results	19
App.2.i SEM-EDX, Raman microscopy and PLM analysis	20
App.2.ii Fourier Transform Infrared Spectroscopy-Attenuated Total Reflectance (FTIR-ATR)	21
App.2.iii Gas Chromatography Mass Spectrometry (GCMS) Analysis	22
App.2.iv SYPRO® Ruby protein staining	23
App.2.v Fibre Identification of the Canvas	23
App.2.vi Radiocarbon measurement	23
App.3 Imaging methods	25
App.4 Plates	26
App.5 Cross-sections	39

Tables, Figures and Plates

Table App.1.i Samples taken for analysis	18
Table App.2.i Analytical results SEM-EDX, Raman Microscopy and PLM	20
Table App.2.ii Summary results from FTIR	21
Table App.2.iii Summary results from GCMS	22
Table App.2.iv SYPRO® Ruby stain results, Sample [13].	23
Table App.2.v Canvas fibre identification, Sample [14]	23
Table App.2.vi.i Radiocarbon measurement, sample [14].....	24
Figure App.2.vi.ii Radiocarbon determination.	24
Plate 1. Mikhail Larionov, Rayonistic Sausage and Mackerel, 1912, collection Museum Ludwig: Inv. Nr. ML 1307. Recto, visible light.....	26
Plate 2. Mikhail Larionov, Rayonistic Sausage and Mackerel, 1912, collection Museum Ludwig: Inv. Nr. ML 1307. Recto, UV light.....	27
Plate 3. Mikhail Larionov, Rayonistic Sausage and Mackerel, 1912, collection Museum Ludwig: Inv. Nr. ML 1307. Recto, raking light.	28
Plate 4. Mikhail Larionov, Rayonistic Sausage and Mackerel, 1912, collection Museum Ludwig: Inv. Nr. ML 1307. Verso, visible light.....	29
Plate 5. Mikhail Larionov, Rayonistic Sausage and Mackerel, 1912, collection Museum Ludwig: Inv. Nr. ML 1307. Verso, UV light.	30
Plate 6. Mikhail Larionov, Rayonistic Sausage and Mackerel, 1912, collection Museum Ludwig: Inv. Nr. ML 1307. Recto, SWIR image.	31
Plate 7a. Mikhail Larionov, Rayonistic Sausage and Mackerel, 1912, collection Museum Ludwig: Inv. Nr. ML 1307. X-ray image.	32
Plate 8.a Maps showing variation in canvas thread angle.....	33
Plate 8.b Histogram of vertical thread count readings.	34

Plate 8.c Histogram of horizontal thread count readings.....	34
Plate 8.d Table of thread count data (threads per centimetre)	34
Plate 9.a Detail of canvas, verso.	35
Plate 9.b Detail of right tacking margin.	35
Plate 9.c Detail of bottom tacking margin.	35
Plate 10.a Macro detail of the priming, recto.....	36
Plate 10.b Detail of exposed priming, recto.....	36
Plate 10.c Detail of canvas, with priming penetrating through, verso.....	36
Plate 11.a Detail of paint surface, recto.	37
Plate 11.b Macro detail of paint surface, showing application of many colours on a single brush...37	
Plate 11.c Detail of paint surface.	37
Plate 12. Image showing approximate location of samples taken for materials analysis.	38
Plate 13. Cross section, Sample [12].....	39
Plate 14. Cross section, Sample [12].....	39
Plate 15. Cross section, Sample [13].....	40
Plate 16. Cross section, Sample [13].....	40
Plate 17. Cross section, Sample [13], stained with SYPRO [®] Ruby.	41

A. Introduction

The painting known as *Rayonistic Sausage and Mackerel* (*Saucisson et maquereaux rayonnistes*)¹ (**Plate 1**) by the artist Mikhail Larionov (1881-1964), a work on a woven support measuring 460 mm high by 610 mm wide, is now part of the collection of the Museum Ludwig, Cologne (Inv. ML 1307). It is unsigned and undated; a date of 1912 has been proposed for its creation. It has been examined as part of a larger technical study of fourteen paintings by Goncharova and Mikhail Larionov in the Museum Ludwig, as part of a project funded through a grant from the charity The Russian Avant Garde Research Project (RARP). The project goal has been to generate detailed technical profiles on authentic paintings by Goncharova and Larionov to expand the data available for art historical study and technical characterization of their work²; consequently, fourteen well-provenanced paintings by the Russian artist couple held in the collection of the Museum Ludwig were thoroughly examined and analysed³. The short-term goal of the project was to define a blueprint for promising routes of research to develop further on other works by these artists and with a long-term goal of contributing such information to support a technical *catalogue raisonné*; these recommendations are laid out in a summary report⁴.

The information in this report therefore provides a detailed technical and material account of the painting. In addition, this is considered in light of the conservation history and provenance information relating to the painting, held by the Museum Ludwig; the supplementary reports produced by Verena Franken in the course of her work on the RARP project summarises this material⁵. Some of the information concerning examination of the painting has been included here, as relevant, as are a representative selection of the extensive documentation photographs she made.

¹ The title of the painting is written on the verso, in Russian and in French: *Lučistaja kolbasa I skumbrija/ Saucisson et maquereaux rayonnistes*. This title was first noted in the catalogue of the sixth exhibition 'The Union of Youth' in 1913. Baudin, K. (ed.) *Der Kubofuturismus und der Aufbruch der Moderne in Russland. Russische Avantgarde im Museum Ludwig*. Museum Ludwig/Wienand: Cologne (2010) p. 77, note 2. Art historical research at the Museum Ludwig revealed that the title of the painting had been recorded as *Rayonistic Sausage and Mackerel* and needed to be changed to *Rayonistic Sausage and Mackerel*. In the past, the title has been translated incorrectly in several sources.

² There is limited specific information available. This includes: Rioux, J.-P.; Aitken, G.; Duval, A. 'Étude en laboratoire des peintures de Gontcharova et Larionov', pp. 220-223. In: *Nathalie Gontcharova, Michel Larionov* [exh. cat.], Éditions du Centre Pompidou: Paris (1995). Rioux, J.-P.; Aitken, G.; Duval, A. 'Matériaux et techniques des peintures de Nathalie S. Gontcharova et Michel F. Larionov du Musée national d'art moderne', *Techne* 8 (1998) 7-32. Gallone, A. 'Œuvres de Michel Larionov et Nathalie Gontcharova: Analyse de la Couleur', *Le dessin sous-jacent la technologie dans la peinture: Colloque XI 14-16 septembre 1995*, R. Van Schoute and H. Verougstraete (eds), Louvain-la-Neuve (1997) pp. 137-141, Pl. 74-76.

³ These include: Natalia Goncharova: *Paysage de Tiraspol (Tiraspol Landscape)*, 1905, ML 01483; *Rusalka*, 1908, ML 1304; *Still Life with Tiger Skin*, 1908, ML 1305; *The Jewish Family*, 1912, ML 1369; *The Orange Seller*, 1916, ML 1484; *Portrait of Larionov*, 1913, ML 1319.

Mikhail Larionov, *Still Life with Coffee Pot*, c. 1906, ML 01486; *Still Life*, c. 1907/1912, ML 1487; *Still Life with a Crayfish (Nature morte à l'écrevisse)*, c. 1907, ML 1331; *Portrait of a Man (Anton Beswal)*, c. 1910, ML 1306; *Rayonism, Red and Blue (Beach)*, 1911, ML 1333; *Saucisson et maquereau rayonnists (Rayonistic Sausage and Mackerel)*, 1912, ML 1307; *Venus*, 1912, ML 1332; *Rayonistic Composition*, inscribed 1916, ML/Z 211/134.

⁴ *Summary Report of the RARP Goncharova/Larionov Project, with the Museum Ludwig*, Art Analysis & Research Inc. (2017).

⁵ See reports: *AAR0955.L ML 1307 Conservation*, Franken, V. 'Report on the examination of the painting *Rayonistic Sausage and Mackerel* (1912) by Mikhail Larionov' (2017a) and *AAR0955.L ML 1307 Archives*, Franken, V. 'Report on the content of the Museum Ludwig archives, concerning the painting *Rayonistic Sausage and Mackerel* (1912) by Mikhail Larionov' (2017b).

The structure of this report is as follows. First, the primary findings of the visual examination and technical imaging will be described in **Section B**.

Materials analysis on micro-samples taken for pigment and binding medium identification and cross-sections is described in **Section C**.

Inferences drawn regarding the painting on the basis of these investigations will be discussed in **Section D**.

The methodologies and protocols used in each case may be found described in the general **Protocols** supplement, appended to this series of reports.

B. Examination, imaging and analysis of the images

B.1 Methodology

The painting was first examined visually under normal lighting conditions and with ultraviolet light (UV), then with a stereo binocular microscope.

A range of technical imaging techniques were also employed (**Appendix 3**), generating a variety of images and imaging datasets⁶. These are presented as follows:

- High-resolution visible colour (**Plate 1**);
- UV luminescence (**Plate 2**);
- Oblique illumination (**Plate 3**);
- Short-wave infrared (SWIR), 1600-2500nm (**Plate 6**);
- X-radiography (**Plate 7**).

Additionally, weave analysis (including thread counting) was conducted on the basis of the X-radiograph (**Plates 8.a-d**). Some exemplar images recorded as part of the surface microscopy and macrophotography are also reproduced here (**Plates 9-11**).

The imaging revealed a range of aspects regarding the use of materials, structure and technique of production of the painting that are complementary to the visual observations made. Consequently, specific observation will be made to each in this section regarding the interpretation of these specific forms of analysis, while a summary overview in the context of the painting technique is presented in **Section D**, below.

⁶ Additionally, a visible-NIR multispectral dataset was collected to examine its suitability for study of paintings of Goncharova and Larionov. As it did not offer information significantly different or superior to that derived by the SWIR imaging, this has not been otherwise reproduced or further analysed here but is available for extramural studies in the future.

B.2 General observations

The painting is executed on a rough canvas, which has not been lined, so that both the recto and the verso of the artwork could be studied. It is not, however, on its original stretcher, having been restretched onto a newer secondary support that appears to be of equal size to the original. The painting is in good condition, with only minor, localised retouching where there have been small losses of paint, particularly along the edges.

B.3 Imaging

Each form of imaging offers different types of insight into the various material aspects of the painting. The most relevant are introduced, in brief, here.

B.3.i Photography with ultraviolet illumination

Excitation by ultraviolet (UV) light can induce luminescence⁷ in some materials, commonly seen as a weak re-emission of light in the visible region. Many natural varnishes have this property, emitting a characteristic weak greenish luminescence. While some pigments (notably zinc white and certain 'lake' pigments) are also active in this way, paints otherwise often do not luminesce. Because of the luminescence of varnishes, which are typically applied as a continuous coating across the surface of a painting, this can provide a means of determining if any disturbance has occurred, such as partial cleaning of the surface or addition of later restoration, where the changes show in contrast to the luminescent areas. Consequently, UV light is commonly used to reveal the presence of retouching. When paintings are not varnished, as is the case here, differences between the colour of the luminescence of the different paints and any added retouching paints can also indicate later stages of intervention (as here; **Protocol 3.2** and **Plate 2**).

In the UV image of this work, small dark areas representing retouched losses of paint may be noted along the right side and lower edge of the art work. No strong luminescence was noted from any of the original paints. What becomes clear in UV illumination is the extent to which the zinc white-based priming has been left exposed, due to the yellowish fluorescence it displays. UV illumination of the reverse equally renders the extent to which it has penetrated to the verso of the canvas (**Plate 5**). As the concentration is clearly thicker around the stretcher bars, the fact that this phenomenon may be observed on all four sides suggests that the original stretcher bars were than those of the current stretcher (originally c. 65 mm; the current bars are 50 mm wide). In the middle field, a lighter, more even penetration is noted, where only tiny amounts of the priming are visible in the small interstices between threads, not substantial penetration as around the edges.

⁷ Commonly referred to as 'UV fluorescence', the word *luminescence* is used here as a broader term that may encompass not only fluorescence phenomena (prompt re-emission of light), but also phosphorescence (slow re-emission of light due to transition via forbidden quantum states). In both cases emission is typically at longer wavelengths than the excitation; here, the excitation is in the UV to blue part of the spectrum (hence 'UV'; in practice, so-called UV-A) and emission in the visible region.

B.3.ii Short-wave infrared (SWIR)

The interest in technologies capable of imaging artworks past the red end of the visible spectrum, in the ‘near’ (‘NIR’) or short-wave (‘SWIR’) infrared regions, has primarily developed out of the long-standing application to reflectography, exploiting the phenomenon of variable transparency of paint films at different wavelengths to enable visualisation of features lying beneath the surface. Imaging of underdrawing has been a major contribution to the study of authorship in paintings, permitting a fuller comprehension of artists’ working practices and extending the evidence used in attribution questions. Practical experience (as well as theoretical consideration) has shown that deeper IR cameras can confer additional benefits in terms of penetration to underlying layers; consequently, a system capable of operating in the SWIR region was used here (see **Protocol 3.4; Plate 6**).

In the IR image, no discrete underdrawing can be seen. However, this does not necessarily mean that no underdrawing is present; as imaging of other paintings examined in this project revealed, underdrawings in friable charcoal or dilute carbon black paint were not usually resolved, although examination at magnification showed its presence. The reason for the lack of resolution in IR lies in a number of factors, probably a combination of the thin and diffuse distribution of the material and the IR blocking properties of the thick overlying layers of paint. Thus, in this particular case, the presence or absence of an underdrawing cannot be ascertained with certainty; the canvas was densely covered with paint, allowing for very limited opportunity to find underdrawing in the gaps between adjacent areas of colour.

While it did not resolve an underdrawing, the IR did reveal overlaps of paint areas; though for the most part, the various fields of colour and line are painted discretely, there are overlaps in some areas, indicating how the composition was built up. The tails of the mackerel, for example, overlap the edge of the box they are placed in, and the brown mass of the sausage, in part.

B.3.iii X-radiography and weave analysis

X-radiography shows internal structures in paintings because the transmitted X-rays are blocked to different degrees by virtue of the inherent absorption and thickness variations of the constituent materials. For example, pigments based on lead (such as ‘lead white’) stop the passage of X-rays more effectively than materials based on organic compounds (such as carbon blacks or the binding medium of the paint), while a thicker application of a material will block more than a thinner one. This allows visualisation of sub-surface features, such as abandoned or altered earlier phases (*pentimenti*), use of techniques such as superimposed forms as opposed to forms left in reserve, characteristic brushwork and so forth.

Here, the prepared surface of the canvas is largely covered by the application of paint, which extends to the tacking margins, although small areas of ground are visible throughout the painting where forms abut. Consequently, the X-ray (**Protocol 3.6; Plates 7.a-b**) reveals a very direct rendition of form, with areas painted in reserve imaging brightly (where they block the passage of X-ray energy), with dark areas around many of these forms, which are painted thinly, or where the canvas is left bare allowing for the easier passage of X-ray

energy. The dark areas corresponding to the thinly primed areas of canvas that were left visible (i.e. unpainted; these are more X-ray transparent than heavily worked regions), which may also be seen in the UV image (**Plate 2**) where these areas of ground display a yellow toned luminescence.

Infilling of the interstices of the threads comprising the canvas support with the priming (ground) also allows the canvas weave to be easily visualised in the X-ray (without the presence of the zinc containing ground, the carbon-based canvas would not be well resolved). Even if a painting is lined, making direct access to the original canvas difficult or impossible, X-ray images can permit the primary weave structure to be examined in detail. A common characterisation of canvases (apart from weave type) cited in the study of paintings is the ‘thread count’, or number of threads per unit in warp and weft directions. Conventionally determined by hand-measuring a number of representative areas, this is now done by applying an image processing algorithm to the entire X-ray image, which has the benefit of providing both greatly enhanced determination of thread counts as well as density and thread orientation information across the whole painting (see **Protocol 3.7; Plates 8.a-c**).

The thread count on this work was determined 11 threads per centimetre in the vertical direction and 9.6 in the weft. The well-distributed and even cusping distortion around the edges of the canvas (**Plate 9.a**) suggests that the painting retains its original format.

C. Sampling and analysis

C.1 Introduction

Samples were taken of the support, ground preparation, paint and varnish layers of the work for analysis by different means in order to determine the range of materials (canvas, pigments, binders and coatings) used in the painting, the nature of the preparation layer and the sequence of layering employed in building up the painting.

To this end, a series of 11 locations selected over a representative range of the painting were micro-sampled for identification of the pigments (**Table App.2.1**), with six micro-samples of paint taken for analysis of the binding media (**Tables App.2.2-2.5**). Two further samples were taken for preparation as cross-sections to study the layering in the selected areas, with the aim of elucidating the development of the painting. Finally, canvas threads were taken for fibre identification and radiocarbon dating.

Micro-samples for analysis were taken from locations that were adjudged to be original (that is, were clearly contiguous with those below and adjacent to them, and not retouching or repair). Locations were also further selected to represent as wide a range of the colours – and therefore probably pigments and media – as possible. Thus, the materials identified and discussed below therefore represent, as far as can be determined, the full extent of the original palette used by the artist.

The micro-samples taken for pigment characterisation were subjected to systematic analysis by polarised light microscopy (PLM) combined with UV-visible-near infrared micro-spectrophotometry, scanning electron microscopy-energy dispersive X-ray spectrometry (SEM-EDX) and Raman microscopy (**App.2.i; Protocols 2.1, 2.2, 2.3**) and some Fourier Transform Infrared Spectroscopy-Attenuated Total Reflectance (FTIR; **App.2.i-2.ii; Protocol 2.4.1**).

Organic components were identified by FTIR and subsequently by Gas Chromatography-Mass Spectrometry (GCMS; **App.2.iii; Protocol 2.5**). Protein staining of cross-sections using SYPRO[®] Ruby was also conducted (**App.2.iv; Protocol 2.6**).

All of the analytical techniques applied are standard methods within the field, capable of allowing the kinds of differentiation required for this type of work. Comparison was also made between samples from the painting and examples of similar pigments from a large collection of reference standards previously analysed by multiple means⁸. Certain differentiations cannot necessarily be made from this range of techniques, although for present purposes the level of discrimination is thought to be largely or wholly sufficient. All materials were generally identified through a combination of the techniques applied; however, certain key diagnostic features were specifically determined through one or other method.

C.2 Support

The canvas was identified as being based on linen (*Linum usitatissimum* L.) in both warp and weft directions (**App.2.v; Protocol 2.7**).

C.3 Radiocarbon dating

Radiocarbon dating was applied to fibres from the canvas support (**App.2.vi; Protocol 2.8**).

The radiocarbon date was determined as 97 years b.p. ± 23 years. After calibration, this yielded a date distribution for which the most relevant period for the origin of the canvas lies 1810-1926 at the 95.4% probability level, pre-dating the so-called 'bomb-pulse' period that begins in the mid-1950s.

C.4 Ground

The ground (Sample [1]) was found to be composed primarily of zinc oxide, combined with minor amounts of calcium sulfate and an aluminosilicate (**App.2.i**). Only protein was detected in association with this layer by FTIR, staining by SYPRO[®] Ruby also proving positive (**App.2.iv**). However, the absence of phosphorus suggests this is unlikely to be casein; it is not possible to

⁸ The pigment reference collection belongs to the Pigmentum Project (see: <http://pigmentum.org>) and runs to around 3500 samples of both historical and modern origin. Analysis of this collection includes PLM and SEM-EDX as well as other techniques such as X-ray diffraction and Raman microscopy. Access to this research collection is gratefully acknowledged. Reference to specific specimens in the text of this report is to the Pigmentum collection number [Pxxxx]. An organic binding media reference collection is also held by AA&R; samples in this set are cited as [AARxxx].

identify the specific nature of the protein based material without further detailed testing, though in the ground, the traditional choice would have been animal-skin glue.

C.5 Underdrawing

No evidence of underdrawing was found in the painting.

C.6 Paint layers: Pigments

The following pigments (**Tables App.2.1, App.2.2**) were identified:

- Zinc oxide ('zinc white')
- Barium sulfate
- Calcium sulfate, gypsum type
- Calcium carbonate, calcite type
- Aluminium hydrate
- Cadmium sulfide ('cadmium yellow')
- Lead chromate oxide ('chrome orange'), with lead sulfate
- CI Pigment Red 3
- Earth pigments of red and yellow tones, containing hematite, goethite and kaolinite
- Ultramarine, synthetic ('ultramarine blue')
- Copper acetate arsenite ('emerald green')
- Carbon-based black as bone coke ('bone' or 'ivory' black)

C.7 Paint layers: Binding media

All paint samples analysed for binding medium using FTIR indicated the presence of a drying oil, with protein additionally detected in Sample [11] (**App.2.ii**). Additional analysis of samples by GCMS indicated that the light yellow-brown paint of Sample [11] contained walnut oil or a mixture of linseed and poppy oils and the white paint of Sample [15] contained poppy oil (**App.2.iii**).

Staining of a cross-section of Sample [13] with SYPRO[®] Ruby indicated that the upper (pinkish brown) paint layer probably also contains some protein (**App.2.iv; Plate 17**).

FTIR also indicated the presence of metal soaps, probably of lead and zinc as well as copper in one instance, assumed to be reaction products between pigments and binding medium.

C.8 Stratigraphy

The preparation of cross-sections allowed for examination of the overall stratigraphy and composition of the priming and paint layers.

Sample [12] (**Plates 13, 14**), taken from blue paint in the upper left corner, shows no discrete ground layer, and canvas fibres can be seen at the base of the sample which luminesce brightly under UV illumination. The lowest pale blue layer consists of white and fine blue particles, and an

occasional red particle, and has a canvas fibre embedded within the layer. Several white areas can also be seen within this layer. The upper blue layer is applied wet-in-wet over the lower blue layer and contains white, blue and black particles.

Sample [13] (**Plates 15-17**), a paint sample from a brown area laid over blue from the top edge, contains a fragmentary white ground layer with embedded canvas fibres. Overlying this is an inhomogeneous blue layer containing blue and white particles, with occasional black and red particles; some large areas of dark red particles can also be seen within this layer. Next, a pale blue layer containing white and blue particles with a few red and black particles is present with, finally, a pale orange-brown layer containing white, red, orange, blue and black particles.

D. Discussion of the findings

D.1 Support, ground and preparatory work

D.1.i The support

The painting has been executed on a medium weight, plain-weave, coarse linen canvas (**Plates 9.a**); no selvedge edges are present. Threads in both directions spun with a z-twist, with thread counts of 11 per cm in the vertical direction and 9.6 per cm in the weft direction (see **Plate 8.a-d**). The weave is somewhat open, with occasional, small interstices found between the threads. This allows both for the penetration of the priming to the verso, in small drops, as well as for a number of interstices to remain open (visible as small ‘holes’ or voids in the canvas; **Plate 11.a**).

The canvas is of a rather rough aspect, suggesting it is not high quality. This is seen by the inclusion of many slubby and irregular threads (**Plates 3, 9.c, 10.c**) in both directions of the weave, as well as numerous bits of linen fibre husk (**Plate 9.a**), indicating that the plant fibres were not carefully cleaned and homogenized before they were spun. The quality of type of material is more consistent with those produced for domestic or industrial use, rather than canvas produced specifically for fine art painting.

As the canvas is unlined, the verso is fully visible (**Plates 4, 5**). It is affixed to a later (non-original) stretcher, primarily by means of round-headed tacks, which are placed in locations near but not identical to the original tacking points (**Plates 9.b, 9.c**) as these have been weakened over time. The earliest label on the stretcher dates to 1967, suggesting a *terminus ante quem* date for the restretching. In some areas, the tacking margins may be seen to extend around the c. 2 cm thickness of the stretcher (**Plate 9.c**) while in others they are a bit narrower.

The stretcher appears to be of the same outer dimensions as the original version (80 x 95.5 cm, bars 7 cm in width), as no noticeable change in dimensions of the painting may be discerned and no cracking associated with the presence of earlier stretcher bars was observed. This is confirmed by the even cusping features found around the edges of the canvas (**Plate**

8.a). The inscriptions and labels present on the verso date to after the painter's death as the stretcher is not original⁹.

D.1.ii Priming

The canvas has been primed with a thin, brittle white ground layer, that appears to have been applied to the stretched canvas by hand, as it conforms to the painting surface but does not extend over the tacking margins (**Plates 9.b, 9.c**). It is composed of zinc oxide, combined with minor amounts of calcium sulfate and an aluminosilicate (**App.2.i**) bound with a protein-based medium (probably animal-skin glue). Its application is thin and irregular and it is quite brittle. The priming does not always fill the interstices between the canvas threads, which are often barely covered by the white application (**Plates 10.b, 11.a**).

There is no evidence that an isolation layer was applied to the canvas before application of the ground; no sign of such a layer was noted by examination under the microscope, nor in the samples prepared as cross-sections. The penetration of small amounts of priming to the verso (and in greater quantity along where the canvas was in contact with the original stretcher bars) further confirms the absence of such a layer (**Plate 10.c**). The thin aspect of the priming may be observed in the cross-sections prepared; Sample [12] (**Plates 13, 14**) does not exhibit a clearly identifiable ground layer, while Sample [13] (**Plates 15-17**) reveals a layer of varying thickness.

Due to the loose, fibrous nature of the canvas and the sparse application of the ground, where visible, the primed support has a very textured, 'furry' aspect (**Plate 10.a**). No attempt appears to have been made by the artist to mask the particularly textured, 'fuzzy', aspect of the canvas by applying a thick ground to smooth it out. Rather, the use of a thin application of priming allows the nature of the support, with its inclusions of slubby fibres and plant husks, to remain visible, providing the painter with a textured, irregular surface on which to paint (**Plate 3**).

D.1.iii Underdrawing

No clear evidence for the use of either underdrawing or underpainting was detected in the examination of the painting, nor in the infrared image that was taken (**Plate 6**).

D.2 Paint, pigments and binding media

D.2.i General observations

The condition of the painting is generally quite good, although there is some minor loss and flaking, predominantly along the right and lower edges (visible in the UV image: **Plate 2**). As noted above, although it is on a new stretcher, it retains its original dimensions.

Both the canvas and the ground might be seen in the context of an artist interested in working on a textured ground, and/or, an artist wanting to save money on supplies. The canvas, likely a

⁹ These are described in more detail in V. Franken, *AAR0955.A 1483 Conservation Report* (2017).

cloth made for domestic or industrial use, not as an artists' canvas, may have provided a cost-effective solution for a painting support. Equally, as the ground is clearly applied by hand – this is not a factory prepared, ready to use painter's canvas – less cost was likely incurred through the choice to mix the zinc white ground and to apply the mixture as part of the process of creation. There is no evidence for the application of the ground onto the tacking edges; it extends only to the edges of the image plane, as does the paint of the composition.

Another piece of evidence that may attest to the artist in savings mode is found in the occasional occurrence of brush hairs in the paint; well-crafted brushes in good condition generally do not lose hairs, while poor quality, or older well used ones are prone to shed. Such inclusions are, however, not excessive, and do not form obvious visual feature. The use of rather wide brushes, evident brushstroke and little concern for smooth transitions and blending, along with the textured aspect of the support, demonstrate a consistent aesthetic in the choice and use of materials.

The painting is executed in a very sure and spontaneous manner apparently without an underdrawing (no evidence of any underdrawing or underpainting was noted, either in the examination with the stereo binocular microscope, nor in the IR image taken; **Plate 6**), suggesting that the shapes were roughly laid in as the artist progressed the composition. Some few areas of overlapping forms may be noted in careful study of the X-ray and UV images (**Plates 6, 7**). The prepared surface of the canvas is largely covered by the application of paint, which extends to the tacking margins, although small areas of ground are visible throughout the painting where forms abut (due to the luminescence of the zinc white preparation layer, this may be clearly seen in the UV image; **Plate 2**). No evidence for complex layering was seen; areas are worked quite directly, with mixing both on the palette, and wet-in-wet directly on the canvas (see cross-sections, **Plates 13-17**). The colours are bright and intense, the paint strongly opaque and used quite thickly as well as spread thinly in other passages. No use of transparent glazes was observed; the colours remain intense, though the surface aspect is quite matte. The painting does not show evidence of having been varnished, in keeping with the artist's preference for a brightly coloured, rough, matte finish.

D.2.ii Paint: pigment and binding medium

The palette used here (**Table 2.i**) is a simple one; one type of pigment has been used for the white (both priming and paint), blue (synthetic ultramarine), green (emerald green) and black (a bone or ivory black). A wider range of warmer tones has been used with cadmium yellow, chrome orange and a red lake (CI Pigment Red 3, with an additive of barium sulfate apparently used in the paint formulation, as it does not occur in any of the other samples) complemented by a range of earth pigments in similar warm tones (containing the minerals yellow goethite and red hematite). Calcium sulfate, calcium carbonate and aluminium hydrate are found as fillers.

The use of an oil binding medium was ascertained for the paints by means of FTIR and GCMS analysis (**App.2.ii, 2.iii**). A white paint sample, Sample [15], was found to be bound with poppy oil, while Sample [11] was found to contain either walnut oil or a mixture of linseed and poppy oil (also supported by the formation of metal soaps in the sample) as well

as some protein, which was confirmed by means of staining with SYPRO[®] Ruby on Sample [13] (**App.2.iv; Plate 17**). Consequently, some form of mixed media was shown to have been used, though the precise nature of the constituent materials cannot be precisely identified with the current techniques.

Given the porosity of the ground and canvas, the fact that there is no staining of the verso of the support that relates to the forms of the composition suggest that the paint is quite leanly bound.

D.2.iii Materials analysis and implications for dating

The painting has been dated to 1912 and was exhibited in 1913¹⁰. None of the material findings presented evidence that would contradict the plausibility of this dating. The radiocarbon measurement of the canvas gave an origin for it between 1810-1926 at the 95.4% probability level, though pre-dating the so-called ‘bomb-pulse’ period that begins in the mid-1950s. In addition to this a period of 3-5 years typically needs to be allowed for processing into canvas and use by the artist, which would still be compatible with the proposed date of 1912. Likewise, the materials otherwise identified in the painting are likewise compatible with the supposed date, although they also continued in use after that time¹¹. The findings generally agree well with the data collected in the study of 45 paintings by Goncharova and Larionov in the collection of the Musée national d’art moderne, Paris¹².

Other technical characteristics arising from the larger review of the works of Goncharova and Larionov may also contribute to a fuller understanding of the relative dating of this painting in the future.

E. Conclusions

The examination of this painting revealed a work that was created with great spontaneity, with a limited palette of materials. The support consists of a coarse linen textile prepared by the artist. The textured aspect of the support was little modified by the addition of the ground (zinc white bound with a proteinaceous medium) which provides a textured field upon which to paint, which is particularly characteristic. This rough aspect is mirrored in the brushwork and handling of the paint. Analytical study of the binding medium revealed a possible use of a mixed media system, whereby an oil paint was modified in some regions of the work by addition of a proteinaceous material. The findings present evidence that is consistent with the proposed dating of 1912.

¹⁰ Baudin, K. (ed.) *Der Kubofuturismus und der Aufbruch der Moderne in Russland. Russische Avantgarde im Museum Ludwig*. Museum Ludwig. Cologne: Wienand (2010) pp. 76, 77 (n. 4). Howard, J. *The Union of Youth: An Artist’s society of the Russian Avant-Garde*. Manchester: Manchester University Press (1992) pp. 141, 150-152. Gordon, D. *Modern Art Exhibitions 1900-1916* (2 volumes), Vol. 1 (1974). Munich: Prestel (1974), p. 709.

¹¹ They would not preclude a revision of date if deemed necessary.

¹² The ground presents the single exception, in that only grounds based on zinc white were noted in those examples prepared by the artists themselves. Rioux, Aitken and Duval (1998) *op. cit.* p. 18.



F. Acknowledgements

Art Analysis & Research would like to thank the following people for their contributions:

Museum Ludwig

Dr Yilmaz Dzewior	Director, Museum Ludwig	
Rita Kestring	Deputy Director, Museum Ludwig	
Petra Mandt	Deputy Head of Conservation, Museum Ludwig	Project coordinator Paintings conservator

Project Team, AA&R

Dr Jilleen Nadolny	Principal Investigator	Project management
Dr Nicholas Eastaugh	Chief Scientist	Materials and data analysis
Bhavini Vaghji	Senior Scientist	Materials analysis
Francis Eastaugh	Senior Imaging Engineer	Scientific imaging processing
Dr Joanna Russell	Scientist	Materials analysis

Project Subcontractors

Verena Franken	Freelance paintings conservator, Cologne, Germany	Project coordinator, examination, documentation and archival research
Patrick Schwarz	Rheinisches Bildarchiv Köln, Cologne, Germany	Photographic documentation
Prof. Hans Portsteffen, Andreas Krupa	Department of Conservation, Cologne University of Applied Sciences, Germany	Capture of X-ray data
Xavier Aure-Calvet	Freelance imaging specialist, Bristol, UK	3D imaging capture and post processing
Prof Haida Liang and team	Nottingham Trent University, UK	Hyperspectral imaging
Dr Irka Hadjas and team	ETH/ Swiss Federal Institute of Technology, Zurich, Switzerland	Radiocarbon analysis

We would also like to extend our sincere thanks to the Peter and Irene Ludwig Foundation and to the RARP donors and to its board of trustees, without whose generosity and vision this project would not have been possible.

G. Appendices

Standard protocols used by AA&R in the preparation of this report for sampling, materials analysis and imaging are listed in each subsection below and detailed in the appendices to the global summary report.

App.1 Sampling and sample preparation

Protocols:

[P.1.1] Sampling

[P.1.2] Cross-sectional analysis

App.1.i Sampling

Table App.1.i Samples taken for analysis				
#	Colour	Description	Location ¹³	Analysis
1		Ground White V. Thin	459/9	PLM, SEM-EDX, Raman, FTIR
2		White	169/57	PLM, SEM-EDX, Raman, FTIR, GCMS
3		Yellow	72/154	PLM, SEM-EDX, Raman
4		Orange	56/107	PLM, SEM-EDX, Raman, FTIR
5		Brown	473/41	PLM, SEM-EDX, Raman, FTIR
6		Crimson Red	546/69	PLM, SEM-EDX, Raman
7		Blue	599/267	PLM, SEM-EDX, Raman
8		Light Blue	457/179	PLM, SEM-EDX, Raman
9		Green	390/81	PLM, SEM-EDX, Raman, FTIR
10		Black	543/307	PLM, SEM-EDX, Raman

¹³ The x/y coordinates in this column are given in millimetres from the left-hand and lower edges of the painting.

Table App.1.i Samples taken for analysis				
<i>#</i>	<i>Colour</i>	<i>Description</i>	<i>Location</i> ¹³	<i>Analysis</i>
11		Light Yellow Brown	450/212	PLM, SEM-EDX, Raman, FTIR, GCMS
12		Blue	0/446	CSA
13		Brown Over Blue	196/462	CSA, SYPRO® Ruby Staining
14		Canvas RHS	0/610	FTIR, C14, Fibre Identification
15		White (as Sample [2])	169/57	GCMS

App.1.ii Cross-sectional analysis

Results are shown in **App.5, Plates 13-17**.

App.2 Materials analysis summary results

Protocols:

- [P.2.1] Polarised light microscopy (PLM)
- [P.2.2] Scanning electron microscopy and energy dispersive X-ray spectrometry (SEM-EDX)
- [P.2.3] Raman microscopy
- [P.2.4.1] Fourier Transform Infrared Spectroscopy-Attenuated Total Reflectance (FTIR-ATR)
- [P.2.5] Gas Chromatography Mass Spectrometry (GCMS)
- [P.2.6] Protein staining with Sypro Ruby©
- [P.2.7] Fibre Identification
- [P.2.8] Radiocarbon dating

App.2.i SEM-EDX, Raman microscopy and PLM analysis

#	Colour	SEM-EDX (elements)			Raman Microscopy (peaks, cm ⁻¹)	Identification
		Major	Minor	Trace		
1	White ground	Zn	S, Ca	Al, Si	1135 (vw), 1008 (w), 668 (vw), 494 (vw), 438 (vw), 414 (vw), 329 (vw)	Zinc oxide (main) ¹⁴ Calcium sulfate, gypsum type (minor) Clay minerals (trace)
2	White	Zn	-	Al, Si, S, Ca	1440 (vw), 1301 (vw), 438 (w), 332 (vw), 274 (vw), 220 (vw)	Zinc oxide ¹⁵
3	Yellow	S, Cd	-	Al, Si, Cl, Zn	311 (vw), 234 (vw)	Cadmium sulfide
4	Orange	Pb	S, Cr, Zn	Al, Si, Ca, Cd	977 (vw), 847 (vs), 837 (vs), 825 (vs), 401 (vw), 381 (w), 356 (w), 342 (m), 324 (w), 279 (vw), 146 (m), 111 (vw)	Lead chromate oxide [P2330] Cadmium sulfide (trace) Zinc oxide
5	Brown	Fe	Al, Si	Mg, P, S, Cl, K, Ca, Ti, Zn, Ba	1583 (w, br), 1302 (w, br), 403 (vw), 295 (vw), 221 (vw)	Hematite (main) ¹⁶ Carbon-based black Aluminosilicate clay minerals (minor)
6	Crimson red	S	Al, Zn, Ba	Si, P, K, Ca, Fe, Sr	1620 (w), 1605 (vw), 1578 (vw), 1554 (vw), 1525 (vw), 1496 (vw), 1445 (w), 1394 (w), 1332 (w), 1320 (vw), 1307 (w, sh), 1256 (vw), 1250 (vw), 1224 (vw), 1216 (vw), 1186 (vw), 1159 (vw), 1129 (vw), 1082 (vw), 1076 (vw), 987 (w), 923 (vw), 842 (vw), 797 (vw), 744 (vw), 723 (vw), 644 (vw), 617 (vw), 502 (vw), 477 (vw), 454 (vw), 421 (vw), 402 (vw), 382 (vw), 340 (vw), 255 (vw), 196 (vw)	CI Pigment Red 3 [P1531] Barium sulfate Zinc oxide
7	Blue	-	Na, Al, Si, S	P, K, Ca, Fe, Zn, Ba	581 (vw), 547 (m), 376 (vw), 254 (vw)	Ultramarine Zinc oxide
8	Light blue ¹⁷	Na, Zn	Al	Si, P, S, Cl, Ca	1597 (w, br), 1305 (w, br), 546 (vw), 438 (vw)	Ultramarine Carbon-based black Zinc oxide

¹⁴ Coarse irregular particles.

¹⁵ Finer particle morphology than sample [1].

¹⁶ Coarse particles. Possibly also from thermal alteration.

¹⁷ Black pigments were observed.

Table App.2.i Analytical results SEM-EDX, Raman Microscopy and PLM

#	Colour	SEM-EDX (elements)			Raman Microscopy (peaks, cm ⁻¹)	Identification
		Major	Minor	Trace		
9	Green	As	Al, Cu	Si, S, Ca, Cr, Zn, Ba	1578 (w, br), 1305 (w, br), 949 (vw), 761 (vw), 540 (vw), 425 (vw), 369 (vw), 326 (vw), 241 (vw), 217 (vw), 174 (vw), 153 (vw), 120 (vw)	Copper acetate arsenite [P1302] Carbon-based black
10	Black	P, Ca	-	Na, Mg, Al, Si, S, Cl, Zn	1580 (w, br), 1307 (w, br)	Carbon-based black (bone or ivory black) (main) Ultramarine (trace) Zinc oxide (trace)
11	Light yellow-brown	Fe	Al, Si	P, S, K, Ca, Ti, Zn	2006 (vw), 1592 (w, br), 1289 (w, br), 546 (vw), 481 (vw), 395 (m), 300 (w), 246 (vw), 145 (vw)	Goethite (main) ¹⁸ Carbon-based black Aluminium silicate clay minerals (minor)

App.2.ii Fourier Transform Infrared Spectroscopy-Attenuated Total Reflectance (FTIR-ATR)

Table App.2.ii Summary results from FTIR

#	Colour	FTIR (peaks, cm ⁻¹)	Identification
1	White ground	3389 (vw, br), 2918 (vw), 2855 (vw), 1636 (vw), 1541 (vw), 1115 (s), 669 (m)	Calcium sulfate, gypsum type Protein
2	White	3365 (m, br), 2918 (m), 2850 (w), 1734 (m), 1716 (vw), 1582 (vw, sh), 1574 (vw), 1568 (vw), 1558 (vw), 1543 (s), 1509 (w), 1456 (m), 1417 (s), 1376 (vw), 1363 (vw), 1316 (vw), 1159 (w), 1105 (vw), 878 (vw), 798 (vw), 670 (vw)	Calcium carbonate, calcite type Oil Metal soap formation, zinc-based ¹⁹ Metal soap formation
4	Orange	2916 (vw), 2849 (vw), 1734 (vw), 1541 (vw), 1457 (vw), 1165 (vw), 1053 (w), 1038 (w), 967 (vw), 841 (m), 627 (vw)	Lead chromate oxide [P2330] Lead sulfate Oil Metal soap formation, presumably lead-based

¹⁸ As earth.

¹⁹ The peaks present in the sample spectrum matched the reference spectrum of zinc stearate, reference number AAR308. Zinc was identified in the SEM-EDX analysis.

#	Colour	FTIR (peaks, cm ⁻¹)	Identification
5	Brown	3691 (w), 3651 (vw), 3619 (vw), 3136 (vw, br) , 2953 (vw, sh), 2917 (m), 2849 (m), 1736 (m), 1719 (vw), 1590 (w, sh) , 1537 (s), 1456 (m) , 1409 (vw), 1399 (m), 1321 (vw), 1163 (w), 1086 (vw, sh), 1028 (s), 1006 (s), 938 (vw), 911 (s), 796 (vw) , 746 (vw), 720 (vw) , 694 (w, sh), 669 (vw)	Aluminosilicate clay mineral, kaolinite type Goethite Oil Metal soap formation, zinc-based ²⁰ Metal soap formation
9	Green	3364 (m, br), 2920 (w), 2852 (vw), 1734 (w), 1715 (vw), 1615 (vw) , 1554 (s) , 1451 (s) , 1417 (m), 1160 (vw, sh), 1092 (m), 1026 (vw) , 816 (m) , 761 (s) , 689 (vw), 633 (s)	Copper acetate arsenite [P1302] Alumina hydrate [P2128] ²¹ Oil Metal soap formation, presumably copper-based ²²
11	Light yellow-brown	3688 (m), 3647 (vw), 3618 (w), 3119 (w, br) , 2920 (vw), 2852 (vw), 1732 (w), 1714 (vw), 1645 (w) , 1634 (vw) , 1549 (w) , 1455 (w) , 1411 (vw) , 1363 (w, sh), 1320 (vw) , 1261 (vw), 1165 (vw) , 1113 (m) , 1081 (vw, sh), 1028 (s), 1003 (s) , 935 (vw, sh), 908 (s), 791 (m) , 752 (w), 668 (m)	Aluminosilicate clay mineral, kaolinite type Goethite Oil Protein

App.2.iii Gas Chromatography Mass Spectrometry (GCMS) Analysis

Sample #	Hexadecanoic acid, methyl ester (C ₁₇ H ₃₄ O ₂)		Octadecanoic acid, methyl ester (C ₁₉ H ₃₈ O ₂)		Ratio
	Retention time, mins	Peak area	Retention time, mins	Peak area	
11	25.678	7.623 x 10 ⁸	29.605	2.898 x 10 ⁸	P/S = 2.63
15	25.643	1.006 x 10 ⁹	29.547	2.706 x 10 ⁸	P/S = 3.72

The P/S value of **Sample [11]**, light yellow-brown paint, was 2.63, consistent with **walnut oil or a mixture of linseed and poppy oil**²³.

The P/S value of **Sample [15]**, white paint, was 3.72, consistent with **poppy oil**.

²⁰ The peaks present in the sample spectrum matched the reference spectrum of zinc stearate, reference number AAR308. Zinc was identified in the SEM-EDX analysis.

²¹ Minor amounts of aluminium were identified in the SEM-EDX analyses.

²² It is assumed that the metal soap present in the sample is copper-based since copper acetate arsenite was the main component identified in the sample.

²³ Other oils whose spectral profile might be considered as matching could include non-traditional examples such as safflower or soybean oil; however, in the present context, this is highly unlikely.

App.2.iv SYPRO[®] Ruby protein staining

Table App.2.iv SYPRO[®] Ruby stain results, Sample [13]²⁴.				
<i>Layer</i>	<i>EDX</i>	<i>FTIR</i>	<i>SYPRO[®] Ruby stain</i>	<i>Interpretation</i>
Ground	Zn S, Ca Al, Si	Protein	Pink staining of ground layer, revealing embedded fibres	Protein in ground
Paint	n.a.	Oil in white, orange, brown, green. Oil and protein in light yellow-brown	Strong pink staining of all paint layers – orange-brown, light and dark blue. Staining appears particularly strong around edges of sample	Protein in paint layers

App.2.v Fibre Identification of the Canvas

Table App.2.v Canvas fibre identification, Sample [14]		
<i>Sample</i>	<i>Observations under PLM</i>	<i>Interpretation</i>
Vertical	Nodes across fibres, parallel extinction, s-twist? One fragment of a blue fibre, knotted? A few structures with low birefringence, some appearing as broadened ends of fibres	Bast fibre, probably linen (<i>Linum usitatissimum</i> L.)
Horizontal	Nodes across fibres, parallel extinction, s-twist. structures with low birefringence as above	Bast fibre, probably linen (<i>Linum usitatissimum</i> L.)

App.2.vi Radiocarbon measurement

Radiocarbon dating is a method for determining age estimates of formerly living organic materials²⁵. Carbon has three naturally occurring isotopes, ¹²C, ¹³C and ¹⁴C. Both ¹²C and ¹³C are stable, but ¹⁴C decays by very weak beta decay to nitrogen (¹⁴N) with a half-life of approximately 5,730 years. While alive, organic materials continue to exchange carbon with the environment, such that they are in equilibrium. On death, the ¹⁴C component begins to decay, such that over time the relative amount decreases. Measuring the level of ¹⁴C remaining in the material then allows for a date to be estimated. This must be additionally calibrated against natural historical variation in relative ¹⁴C levels in the environment, for which there are accepted standard curves expressing the changes over time²⁶.

²⁴ For the ground layer, EDX and FTIR data derives from separate analysis of another sample.

²⁵ Based on from the websites of the NDT Resource Center, <http://www.ndt-ed.org/EducationResources/CommunityCollege/Radiography/Physics/carbondating.htm> and the website of the Oxford Radiocarbon webinfo site:

<http://c14.arch.ox.ac.uk/embed.php?File=webinfo.html>, both consulted on 3 February 2013.

²⁶ For example, that used here is one known as IntCal13.

Prior to radiocarbon measurement, fibre identification was undertaken and the canvas sample was pre-tested using FTIR to ascertain the presence of any contaminating material that could influence the outcome. As noted elsewhere, the fibre was identified as a bast type, probably linen (*Linum usitatissimum* L.). FTIR indicated the presence possibly an oil in addition to the cellulose of the fibre²⁷.

The canvas sample was then submitted to the Laboratory of Ion Beam Physics, ETHZ at the Swiss Federal Institute of Technology (*Eidgenössische Technische Hochschule Zürich*) for radiocarbon dating (see **Protocol 2.7**).

Sample-Nr.	Sample Code	Material	C14 age BP	$\pm 1\sigma$	F14C	$\pm 1\sigma$	$\delta C13$ ‰	$\pm 1\sigma$	mg C	C/N
ETH-77077	AAR0955.L.14	Textile fibre	97	23	0.988	0.0028	-26.4	1	0.99	197.01

The radiocarbon date was determined as 97 years b.p. ± 23 years. After calibration, this yielded a date distribution for which the most relevant period for the origin of the canvas lies 1810-1926 at the 95.4% probability level, pre-dating the so-called ‘bomb-pulse’ period that begins in the mid-1950s.

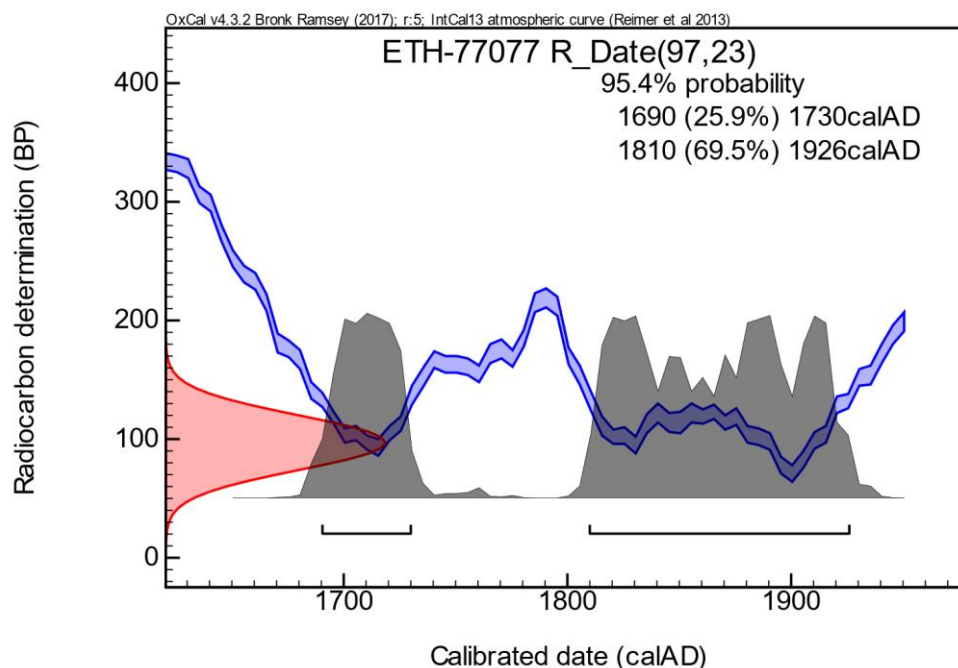


Figure App.2.vi.ii Radiocarbon determination.

²⁷ Non-cellulosic materials are aimed to be removed by the sample pre-treatment process prior to the radiocarbon measurement.



App.3 Imaging methods

Protocols:

- [P.3.1] Photography with visible light
- [P.3.2] Photography with ultraviolet illumination
- [P.3.4] SWIR infrared imaging (IR)
- [P.3.6] X-radiography (X-ray)
- [P.3.7] Thread counting and weave analysis

App.4 Plates



Plate 1. Mikhail Larionov, *Rayonistic Sausage and Mackerel*, 1912, collection Museum Ludwig: Inv. Nr. ML 1307. **Recto, visible light.**

Rheinisches Bildarchiv Köln, Patrick Schwarz, rba_d050876_08, www.kulturelles-erbe-koeln.de/documents/obj/05020024



Plate 2. Mikhail Larionov, *Rayonistic Sausage and Mackerel*, 1912, collection Museum Ludwig: Inv. Nr. ML 1307. **Recto, UV light.**

Rheinisches Bildarchiv Köln, Patrick Schwarz, rba_d050876_06, www.kulturelles-erbe-koeln.de/documents/obj/05020024



Plate 3. Mikhail Larionov, *Rayonistic Sausage and Mackerel*, 1912, collection Museum Ludwig:
Inv. Nr. ML 1307. **Recto, raking light.**

Rheinisches Bildarchiv Köln, Patrick Schwarz, rba_d050876_04, www.kulturelles-erbe-koeln.de/documents/obj/05020024

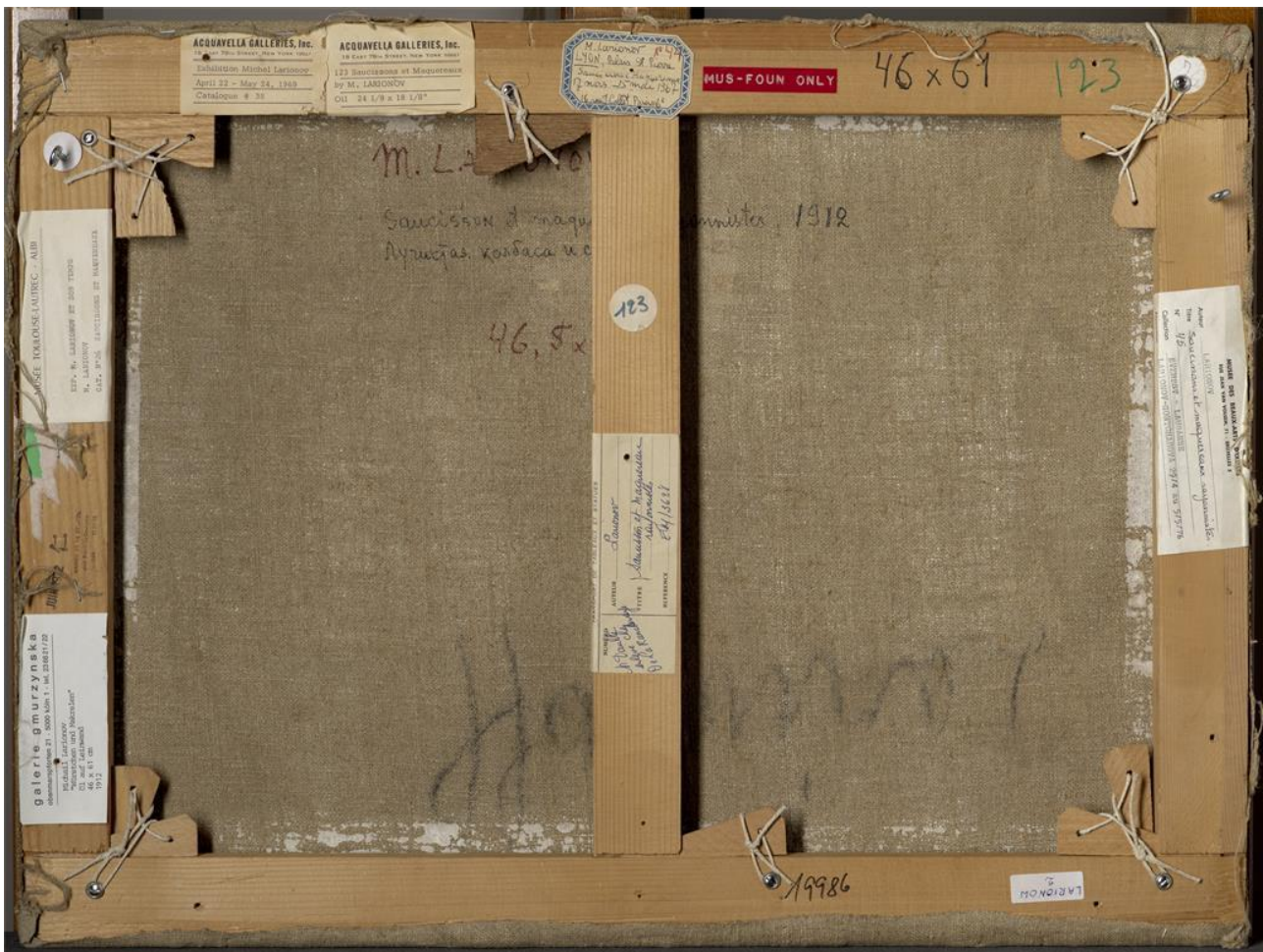


Plate 4. Mikhail Larionov, *Rayonistic Sausage and Mackerel*, 1912, collection Museum Ludwig: Inv. Nr. ML 1307. **Verso, visible light.**

Rheinisches Bildarchiv Köln, Patrick Schwarz, rba_d050876_02, www.kulturelles-erbe-koeln.de/documents/obj/05020024

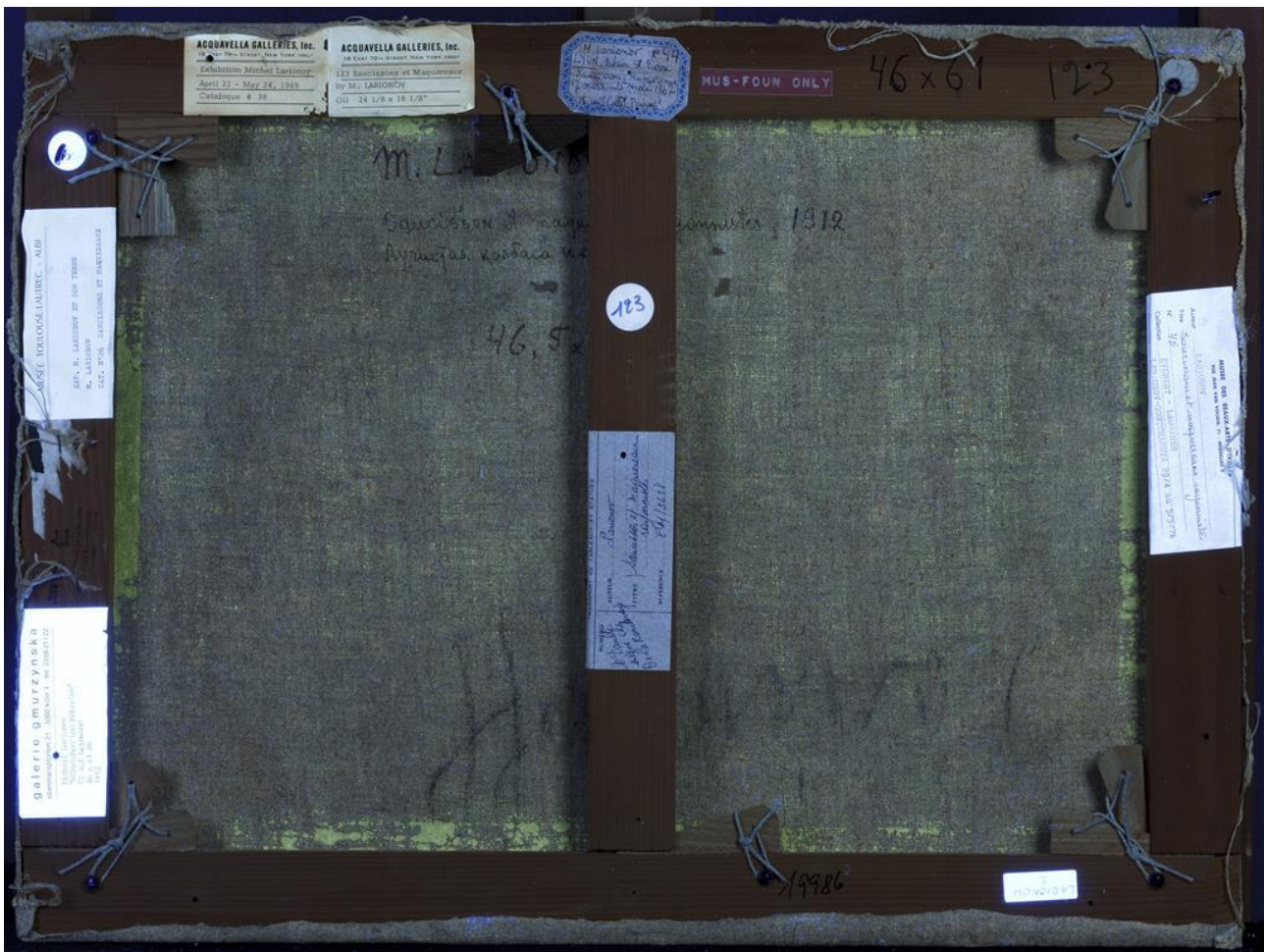


Plate 5. Mikhail Larionov, *Rayonistic Sausage and Mackerel*, 1912, collection Museum Ludwig; Inv. Nr. ML 1307. **Verso, UV light.**

Rheinisches Bildarchiv Köln, Patrick Schwarz, rba_d050876_07, www.kulturelles-erbe-koeln.de/documents/obj/05020024.



Plate 6. Mikhail Larionov, *Rayonistic Sausage and Mackerel*, 1912, collection Museum Ludwig: Inv. Nr. ML 1307. **Recto, SWIR image.**



Visible light image, for comparison. The tails of the mackerel are seen to sit over the paint of the brown sausage, uppermost.

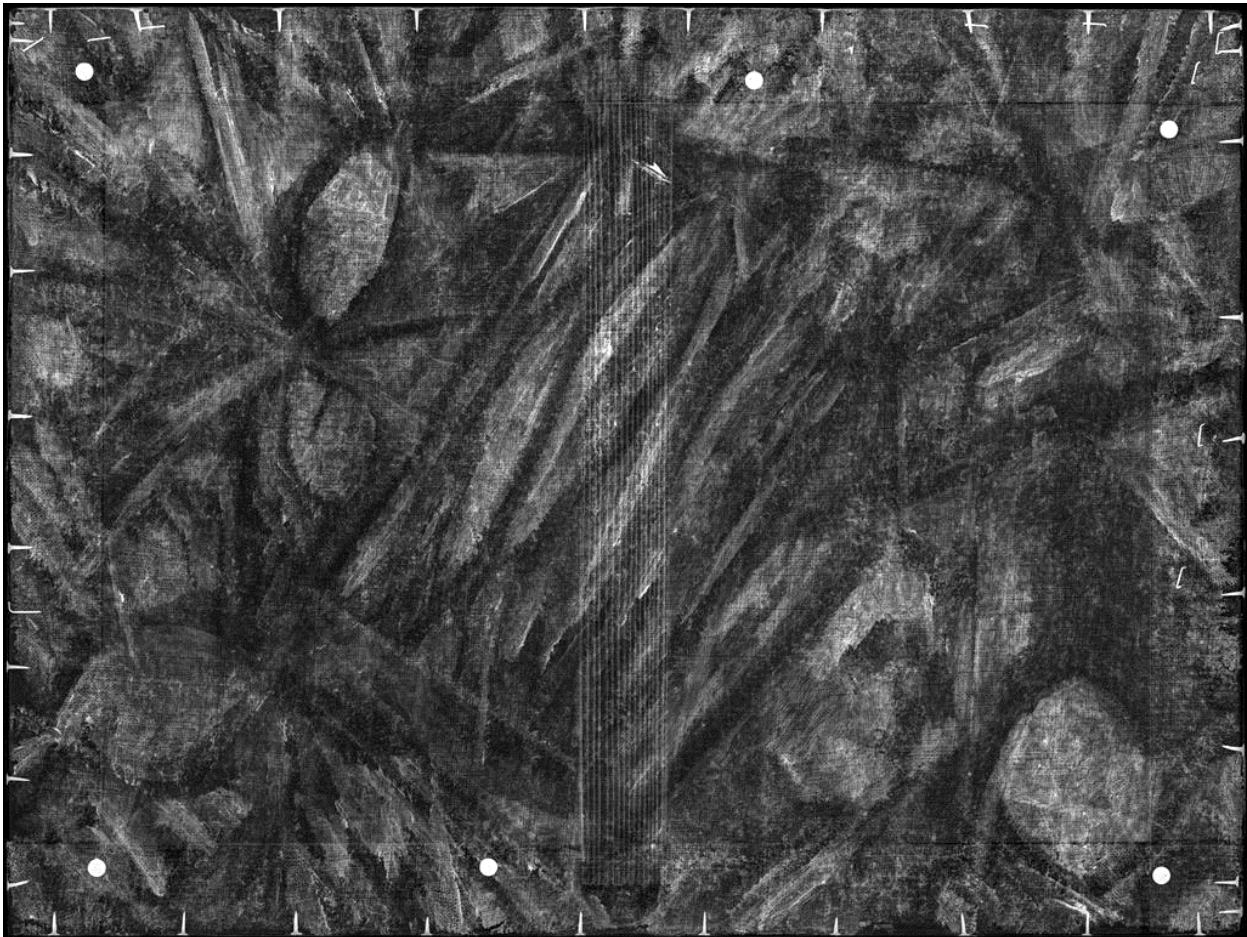
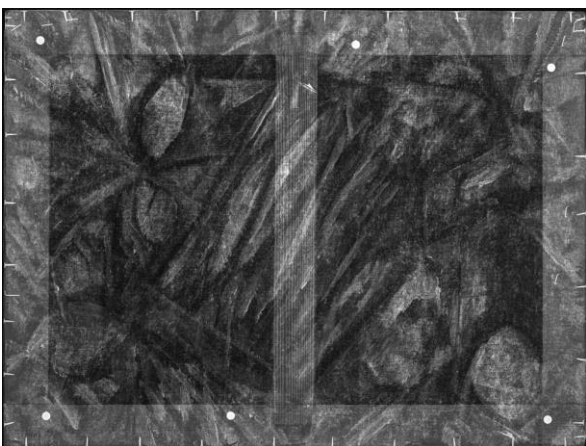


Plate 7a. Mikhail Larionov, *Rayonistic Sausage and Mackerel*, 1912, collection Museum Ludwig; Inv. Nr. ML 1307. **X-ray image.**

Below, **b.**), the X-ray image before digital compensation for the stretcher bars and **c.**), visible light.



7b.



7c.

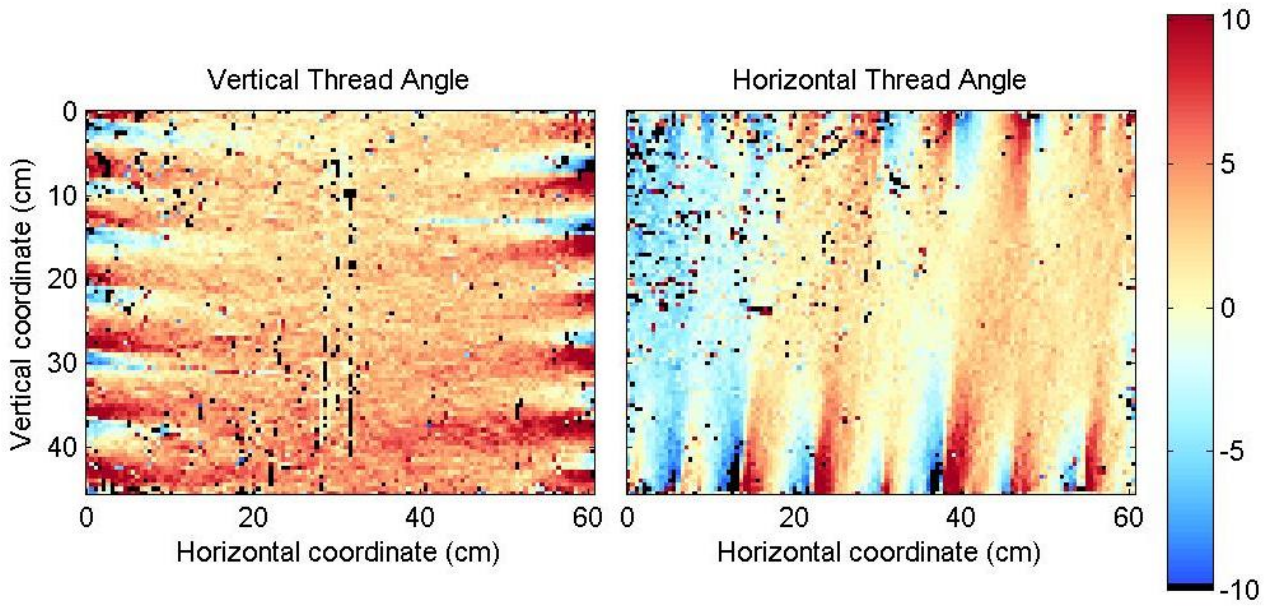


Plate 8.a Maps showing variation in canvas thread angle.

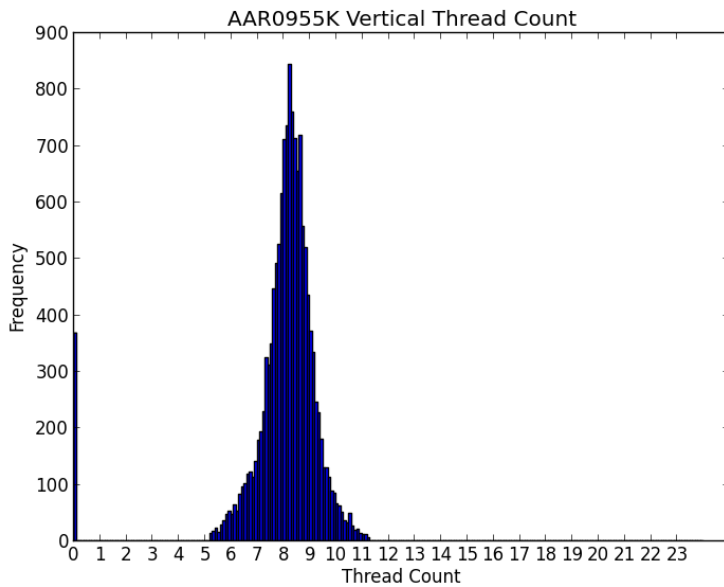


Plate 8.b Histogram of vertical thread count readings.

Showing variation in thread count per centimetre.

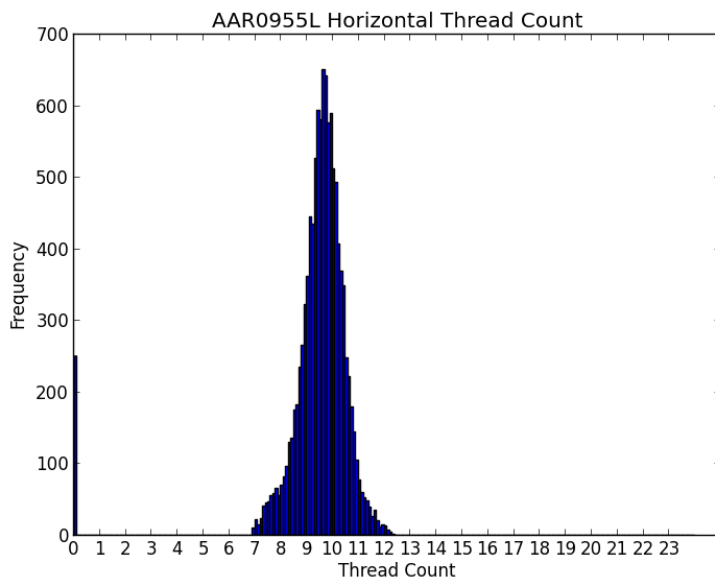


Plate 8.c Histogram of horizontal thread count readings.

Showing variation in thread count per centimetre.

Plate 8.d Table of thread count data (threads per centimetre)		
	Mean	Estimated thread count (mode)
Vertical	10.4	11
Horizontal	9.6	9.6



Plate 9.a Detail of canvas, verso.

The canvas is a thin, plain weave type. No selvedge is present. The fibre type is apparently linen (*Linum usitatissimum* L.). The white priming may be seen to penetrate the canvas and many bits of husk may be seen in the threads.



Plate 9.b Detail of right tacking margin.

The thin, white priming may be seen to stop at the turn over edge and rust marks from former nail holes are visible.



Plate 9.c Detail of bottom tacking margin.

The irregular aspect of the canvas, with numerous slubby thread inclusions may be seen.



Plate 10.a Macro detail of the priming, recto.

It is very thin and porous, barely covering the canvas and allowing the fibres and weave structure to remain fully visible.



Plate 10.b Detail of exposed priming, recto.

The priming is applied very thinly; it does not fill all of the interstices of the canvas, allowing small open holes to remain.



Plate 10.c Detail of canvas, with priming penetrating through, verso.

The priming has seeped through the canvas in strips that relate to the original stretcher bars, which were wider than the current ones.



Plate 11.a Detail of paint surface, recto.

The priming and paint are applied very thinly in some areas; it does not fill all of the interstices of the canvas, allowing small open holes to remain.



Plate 11.b Macro detail of paint surface, showing application of many colours on a single brush.

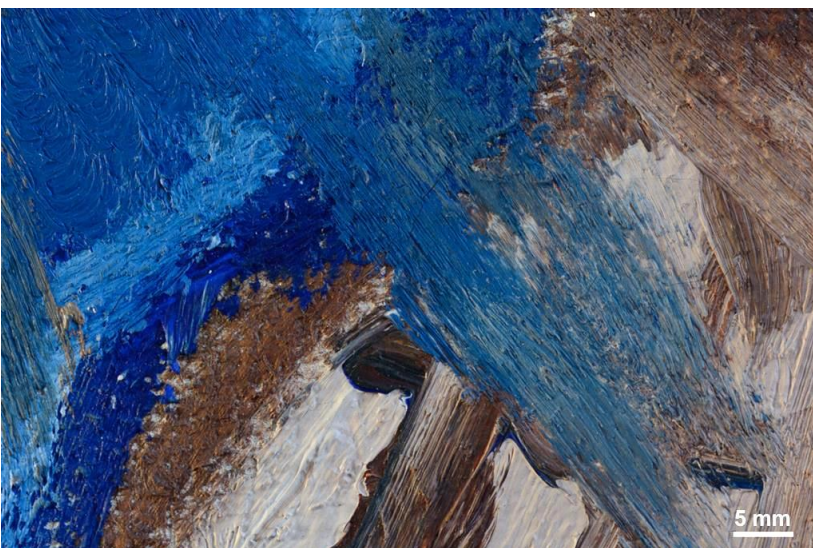


Plate 11.c Detail of paint surface.

Both applications of very fluid, wet in wet paint, as well as dry brush technique are visible.



Plate 12. Image showing approximate location of samples taken for materials analysis.

App.5 Cross-sections²⁸



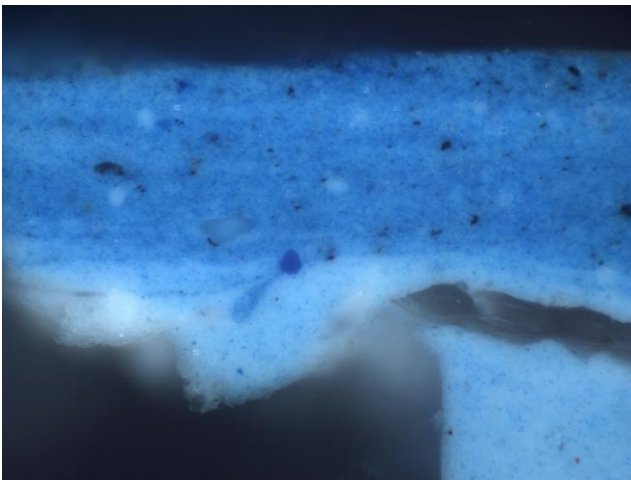
a.



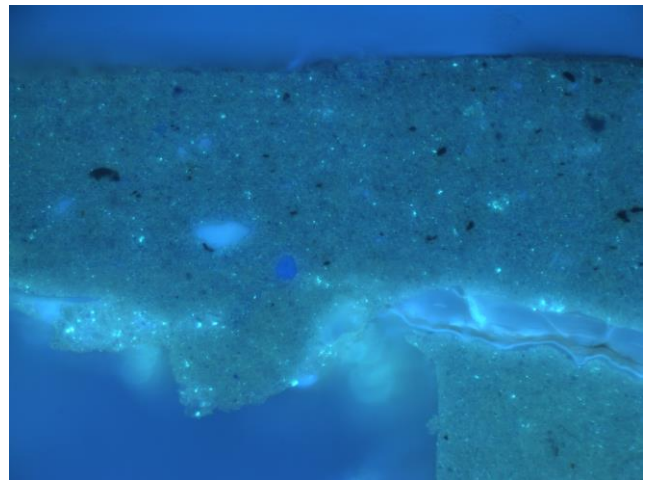
b.

Plate 13. Cross section, Sample [12].

Image ~1mm high. From blue paint in the upper left corner. No discrete ground layer is apparent, but canvas fibres can be seen at the base of the sample which luminesce brightly under UV illumination. The lowest pale blue layer consists of white and fine blue particles, and an occasional red particle, and has a canvas fibre embedded within the layer. Several white areas can also be seen within this layer. The upper blue layer is applied wet-in-wet over the lower blue layer and contains white, blue and black particles.



a.



b.

Plate 14. Cross section, Sample [12].

Image ~260µm high. Detail of Sample [12] from the blue paint at higher magnification, showing the embedded canvas fibre. In all layers speckles of green luminescence characteristic of zinc white can be seen, particularly in the area of white paint.

²⁸ Photographed under visible light, left (a.), and with ultraviolet illumination, right (b.), unless otherwise stated.

*



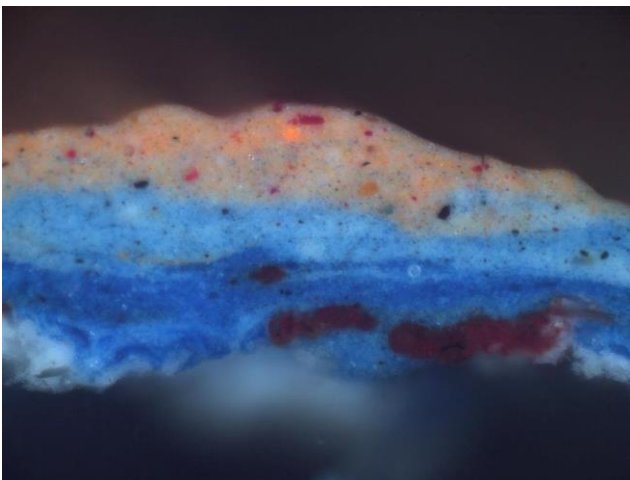
a.



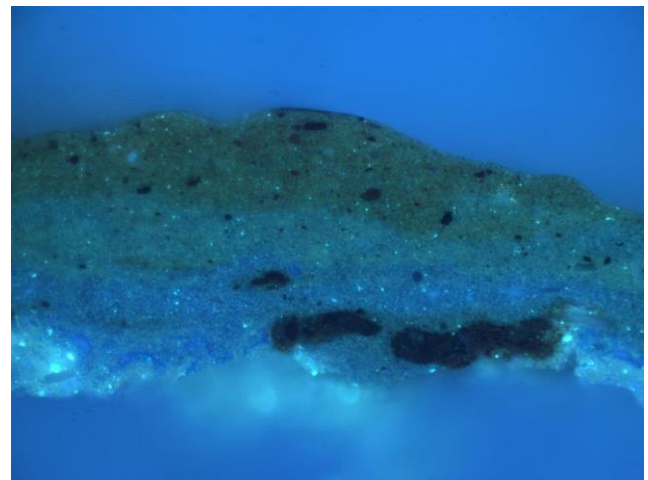
b.

Plate 15. Cross section, Sample [13].

Image ~1mm high. Brown over blue from top edge. Layers from bottom up: 1, a fragmentary white ground layer with embedded canvas fibres; 2, an inhomogeneous blue layer containing blue and white particles, with occasional black and red particles. Some large areas of dark red particles can also be seen within this layer; 3, a pale blue layer containing white and blue particles with a few red and black particles; 4, a pale orange-brown layer containing white, red, orange, blue and black particles.



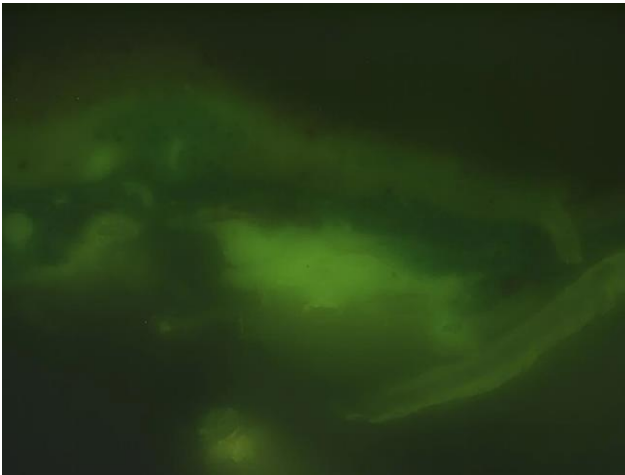
a.



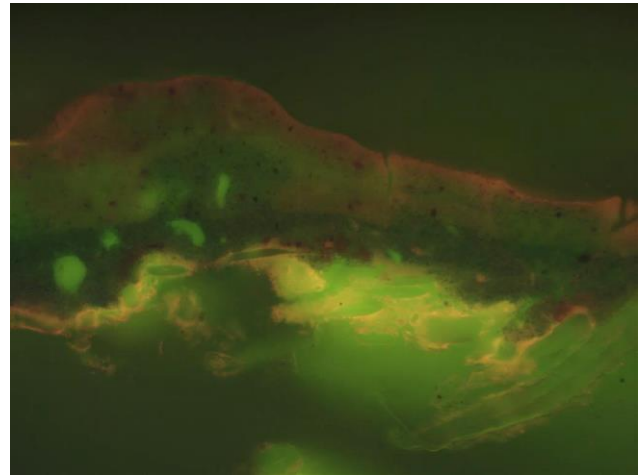
b.

Plate 16. Cross section, Sample [13].

Image ~260µm high. Brown over blue, detail of sample at higher magnification. The bright green luminescence of zinc white in the white ground layer can be clearly seen in the UV image (a small fragment is preserved, left), and scattered particles of similar appearance are also visible throughout the paint layers. The paint layers are intermingled with no distinct boundaries, indicating wet-in-wet paint application.



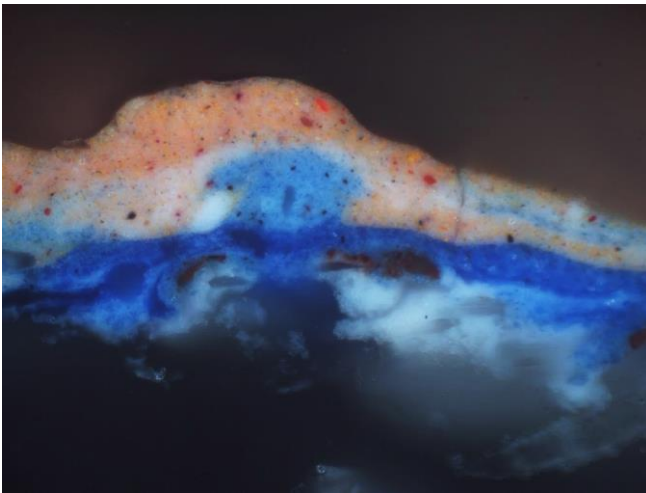
a.



b.

Plate 17. Cross section, Sample [13], stained with SYPRO[®] Ruby.

Image ~260µm high, viewed with Leica I3 filter before (**a.** left) and after (**b.** right) staining (below, **c.** in visible light for comparison). Pink staining of the ground layer is visible (highlighting the embedded fibres), indicating the presence of a protein-based medium in the ground. Additionally, strong pink staining of all paint layers – orange-brown, light and dark blue - also indicates the presence of protein.



c.